International Journal of Scientific Research in Engineering and Management (IJSREM)
Volume: 08 Issue: 11 | Nov- 2024 SJIF Rating: 8.448 ISSN: 2582-3930

"ANALYSIS OF REINFORCED EARTH EMBANKMENT"

Gyanendra Shakya[1] and Prof. Satyendra Mittal[1]

[1]Department of Civil Engineering, Indian institute Of Technology Roorkee.

ABSTRACT- The objective of this study is to find the suitability of finite element method for analysing reinforced embankment on sandy and clayey soil using MIDAS GTS NX modelling software, to carry out the objective, many finite element analysis were carried out on a prototype scale using a 2D 15-noded plane strain element utilizing the computer MIDAS GTS NX code. Then the slope inclination, geogrid spacing variation, vertical spacing of geogrid layer, load variation, and effect of PET and PP geogrid on the behaviour of reinforced sandy and clayey embankment on soil is determined. The length of the geogrid layers (L.) and the vertical spacing between geogrid layers are among the characteristics (S.), the vertical loading on the embankment, the height of embankment were investigated. The stability of a road embankment without reinforcing is examined first, then a series were conducted to study the influence of one parameter while the other parameters were kept stable. The addition of geogrid layers enhances the stability of the loose sand slope, according to numerical analysis of the data. It is also found that the layers of the geogrid become a barrier to the critical failure surface and shift the failure surface to the stronger one, thus increasing the factor of safety (FOS). It is noticed that by increasing the length of reinforcement and increasing the spacing between the reinforcement layers, the safety factor (FS) of the slope decreases with increase of the geogrid spacing.

Keywords: Geotextile, road embankment, numerical analysis, PET (polyester), PP (polypropylene).

1. INTRODUCTION

For the analysis of the earth, geotechnical engineers have used a variety of approaches and techniques. Finite element Method (FEM) based on Cohesion (c) and internal friction angle (ϕ) reduction using the Finite Element Method (FEM). Limit Equilibrium Method (LEM), Finite Difference Method (FDM), Limit Analysis (LA), and a combination of these methods are some of the methods that can be used.

Many researchers have worked hard to figure out how geosynthetics, waste tyre shreds, and other materials affect reinforced soil behaviour. Engineers have looked into shear strength, permeability, compressibility, and modulus of elasticity in reinforced soils (P S. & D. Tjander, 2015). Geogrid layers and geosynthetics can improve the mechanical properties of soils in tension. Geogrid layers are commonly used to increase the stability of soil embankments. On both sides, the reinforcement that holds the soil mass together. FEM-based design analysis for each slope reinforced with geotextile and geogrids were used. The geotextile reinforced embankment must be constructed with sufficient safety and displacement factors. There have been some studies on the use of geotextile reinforcement in soft soil. Analyses must be based on a model that accurately describes site subsurface characteristics, ground behaviour and applied loads over the course of a structure's lifetime, taking into account the environment. To evaluate the outcomes of analysis, judgments on acceptable risk or safety variables must be made. This is a better option if higher shear strength soil is available nearby. When reinforcement was added, the factor of safety and total displacement were found to be lowered, according to the study's findings. The performance of geogrid reinforced slopes was investigated by an experimental and numerical analysis. After applying dynamic loads, failure surfaces and deformations were observed in their investigation. Geogrid layers were found to have stronger strength and less deformation than geotextiles. To better understand the slope failure mechanism, several researchers analysed a few case studies of slope failure and did static and dynamic analysis using numerical analysis, which they compared to analytical approaches. (Akbas, 2015), (Alemdag, et al., 2015) (Awalla, et al., 2020) (Gor, 2021).

The purpose of this study is to determine the optimum angle of road embankment considering the allowable FOS and displacement at different types of loading (variable) and to determine stability analysis of the road embankment by FEM using MIDAS GTS NX.

The parameters investigated are geogrid length, vertical spacing between geogrid layers, variation of embankment angle and load variation.

Road embankment:

According to AASHTO, the world's oldest road, "The Royal Road," which runs through southwest Asia and Asia Minor, was first used by wheeled vehicles approximately 3000 B.C. (1950). The Ten Books on Building were written by the Romans in the first century B.C.., and it is one of the earliest technical works of soil-based architecture.

The design of the embankment is extremely complex since it is influenced by the project's aim, the surrounding environment, and the ground foundation conditions. When constructing an embankment, engineers must plan ahead, collect geometric data, and assess stability. The road embankment is built up from a series of compacted layers until the subgrade surface level is reached. It's also called a structural embankment, and it's available in two types: unreinforced and reinforced. Its function is to carry traffic loads to the soil base. To achieve the necessary design efficiency, suitable stability assessment and geometric data methodologies are required. This section discusses three major features of geometric data, design and analytical methodologies, based on recent literature.

Figure 1 Road embankment stabilization

Geogrid:

Tensile drawing, sometimes known as "cold working," is a method for creating high-modulus polymer materials that has increased the likelihood of such polymers being used to reinforce soils for walls, steep slopes, roadway bases, and foundation soils. As a result, the primary purpose of these geogrids is to provide reinforcement. This sector, like many others, is thriving, with a diverse range of goods, materials, and connections making up the geogrid industry today. The apertures-the openings between adjacent longitudinal and transverse ribs-must be large enough to allow soil communication, or strike-through, from one side of the geogrid to the other in all geogrids. When match to geotextile fibres, geogrid ribs are frequently stiff. As we'll see later, rib strength is more important, but shown is junction strength. This is because, in some cases, soil strike-through within the apertures bears against the transverse ribs, transferring the load to the longitudinal ribs via the junctions. Of course, the longitudinal and transverse ribs meet and are connected at the connectors. Nodes are second name for them.

Uses of geogrid is repairing slope failures and landslides, As gabions for wall and bridge abutment construction and as three-dimensional mattresses for embankment over soft soils etc.

International Journal of Scientific Research in Engineering and Management (IJSREM)
Volume: 08 Issue: 11 | Nov- 2024 SJIF Rating: 8.448 ISSN: 2582-3930

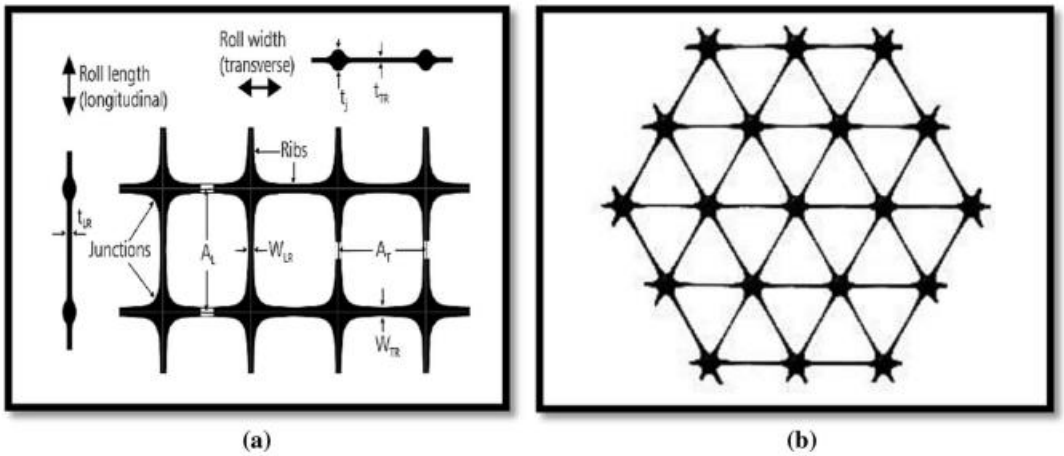

Figure 2 (a) Biaxial geogrid (b) triaxial geogrid (Mittal & Bhardwaj, 2020)

1.2 Objective of the study

The objective of this research is to determine the impact of geosynthetic reinforcement on layered soil modules. This goal was achieved by completing the sub-objective listed below.

i) Numerical studies of geosynthetic reinforced soil road embankment using layered sand strata under the variable loading (UDL)

ii) Response of geosynthetic reinforced soil road embankment made fine soil (layered clay) strata under variable loading (UDL).

1.3 Layout of the thesis written below

The following are the chapters that make up the thesis:

i) Chapter 1: Introduction- This chapter includes background information about geosynthetic reinforced soil embankment and objectives which is intended to achieve with this study.

ii) Chapter 2: Literature review- This chapter reviewed the work done by various researchers on geosynthetic reinforced soil road embankment and different kind of numerical analysis on various types of soil.

iii) Chapter 3: Data and Software- This chapter includes the details of all the datasets and software used for the research.

iv) Chapter 4: Methodology adopted- This chapter provides all the necessary details about the methodology adopted to achieve the objectives of the research.

v) Chapter 5: Result and Discussion- In this chapter, the significance of all the findings have been described.

vi) Chapter 6: Conclusion- In this chapter, all the new insights that emerged as result of this research is explained. This section also includes the limitation of the research and future scope of the study.

LITERATURE STUDIES

In this chapter, various kind of work done by different researchers have been discussed.

2.1 (Wulandari & Tjandra, 2015)

The finite element approach was used to analyse the road embankment's stability using PLAXIS 2D. Three forms of sequence modelling were used in this research. First to investigate the stability of road embankment without any reinforcement. The second modelling step was to identify the length of geotextile reinforcement based on the model road embankment's stability. The final step was to test the stability of the model reinforced embankment with varied geotextile reinforcement tensile strengths.

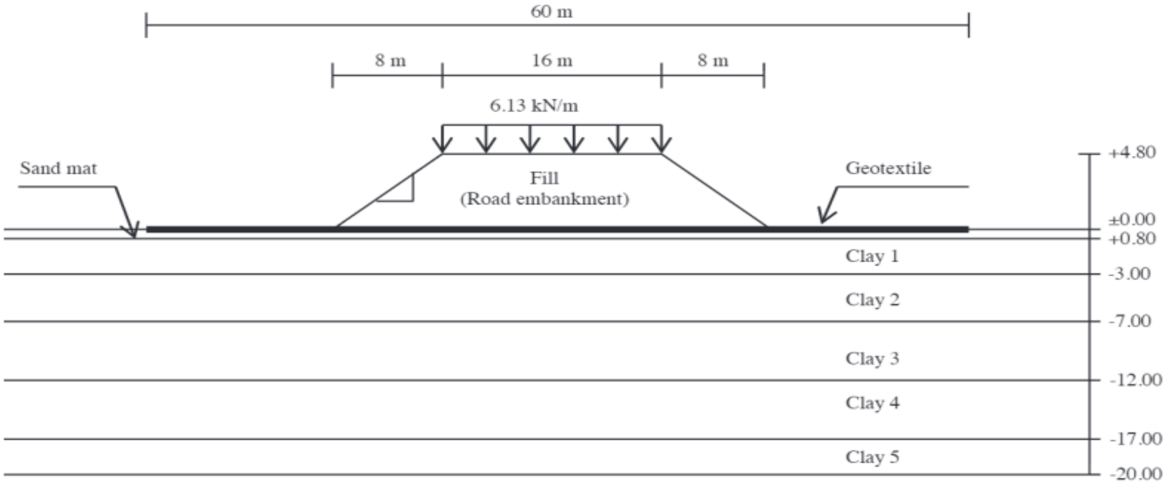

Figure 3 Model geometry (P S. & D. Tjander, 2015)

In this figure (3), the height of the embankment is 4m and the angle of the embankment will be 26.68 with slop as 2H: 1V was investigated in this study. The water table is considered to be at zero level. In preference to traffic load, a notional surcharge of 6.13 kN/m2 was utilised. Also, the layer of geotextile PET woven is placed between the base of the embankment and the sand mat.

Material	γ_{unsat} (KN/m^3)	γ_{sat} (KN/m^3)	E_{ref} (KN/m^3)	C (KN/m^3)	Ø (0°)	φ (0°)
Embankment Fill	18	18	50000	1	33	3
Sand Mat	18	23	30000	1	33	3
Clay layer 1	16.60	17.30	2000	33.02	1	0
Clay layer 2	16.601	17.307	2000	12.01	1	0
Clay layer 3	16.612	17.306	2000	47.07	1	0
Clay layer 4	16.612	17.304	2000	118.66	1	0
Clay layer 5	16.614	17.31	2000	163.45	1	0

Table 1 Soil parameter (P S. & D. Tjander, 2015)

The main objective of this paper is to find out the optimum tensile strength of geotextile as the reinforcement of the road embankment taking into consideration the permissible factor of safety and displacement. The factor of safety improves as the tensile strength of the geotextile reinforcement increases in this investigation, because displacement has no substantial influence on geotextile tensile strength. The result of this research proved that the safety factor has a significant impact on the optimum tensile strength of geotextiles.

2.2 (Mittal & Bhardwaj, 2020)

Geosynthetics are increasingly being used in civil engineering projects. The use of geogrid in stress distribution and displacement reduction is undeniable, and most civil engineering projects have benefited from it. The goal of this research is to better understand the field behaviour of geogrids under heavy loads. As a result, laboratory pull-out tests replicating reinforced railway embankments under large axle loads were done. In the big experimental box, 36 pull-out experiments on biaxial and triaxial geogrids were done to evaluate their behaviour when utilised for railway embankments. The tests were carried out at two distinct strain rates of 5 mm/min and 1 mm/min in order to better understand how strain rate affects the effects of severe stress. The results show that biaxial geogrids are a better solution for high-stress railway applications. When compared to triaxial geogrids, biaxial geogrids provide 33.51 percent greater pull-out resistance and 59.28 percent more elongation (with a tension of 250 kN/m^2). The study also found that triaxial and biaxial geogrids both behave as strain-hardening materials, with biaxial geogrids having a stronger effect.

2.3 (Mesut, et al., 2022)

This research investigates the impact of geogrid layers on the stabilisation of a dry loose sand slope with a dense sand layer beneath it. A series of finite element analyses were performed on a prototype slope using a two-dimensional 15-node plane strain model and the computer PLAXIS 2D code to achieve this goal. The length of the geogrid layers (L), the vertical spacing between geogrid layers (S), and the axial stiffness of the reinforcement (EA) were all investigated. The incorporation of geogrid layers improves the stability of the loose sand slope, according to numerical study results. It also fined that Slope stability is improved by adding layers of geogrid to loose sand slopes.

2.4 (Mwasha, 2009)

In circumstances where short-term reinforcement is required, increased environmental concern has led to the investigation/consideration of employing Limited Life geotextiles as an alternative for man-made materials. The general goal of the research is to create a thorough model of the required strengthening behaviour of Limited Life Geotextiles with a finite (but definable) operating life. To accomplish this, an analytical model for soil reinforcement was developed that takes into account changes in foundation soil strength over time owing to consolidation. A geotextile's tensile tension that ensures a particular Factor of Safety against potential hazards. The failure of an embankment as a function of time and soil conditions was then determined. As a result, the analytical model was effective, demonstrating that geotextiles with short design lives can be used in specific technical applications

DATA AND SOFTWARE

The Strength Reduction Method is used by MIDAS GTS NX, a Finite Element Modelling-based tool, to assess the type and cause of slope collapse. Investigation to finding the strength reduction method, slope strengthening tools can be used to stabilise the slope (Tarun & Vinod K., 2017).

KEYWOEDS: Strength Reduction Method, Finite Element Modelling, MIDAS GTS NX

3.1 INTRODUCTION:

The Strength Reduction Method (SRM) is a finite element analysis technique. Shear Strength Reduction Method (Hammah, 2005) is alternative name for it. The soil is weakened in an elastic-plastic finite element analysis until the slope fails, resulting in stability by strength reduction technique (Bacic & Uljarevic, 2014). The Component of factor of Safety (FOS) is thought to be the factor that causes the soil strength to deteriorate until it fails. Its fundamental notion is to reduce a material's shear strength envelope by a factor of safety before starting a finite element analysis on the slope until the deformations become unacceptable or the solutions do not converge. For a slope with a FOS>1, SRM looks for the crucial factor of safety. Repeated iterations of FEM are carried out using incremental values of factor of safety until the material strength is lowered to the point where the slope breaks (GTS, 2014) (Hamdhan, 2013) (H. Jerry Qi, 2006) (Fernando Alonso, 2013).

3.2 (Tarun & Vinod K., 2017)

1. While considering the types of slop if factor generally known as strength reduction factor (SRM) is calculated and the finite element analysis (FEM) is done through the software.
2. A number of iterations is performed by changing the value of (SRM) strength reduction factor till the soil slope model becomes unstable.
3. Finally, a critical strength reduction factor is identified based upon, factor of safety of soil is determine.

The SRM under-takes Mohr-Coulomb strength (MIDAS, 2014)for slope stability analysis. This is most well-known criteria for failure analysis of slopes in geotechnical engineering. This model is unique in that it can forecast the failure of a given slope.

The working of MIDAS GTS NX is explained in below given steps:
Step (1) Soil sample collection disturbed, and undisturbed soil samples are collected from the land slide site.
Step (2) Engineering properties of soil are identified for classification through the laboratory testing.
Step (3) Three-dimensional modelling through finite element method of slope on GTS NX tool of MIDAS software is performed.
Step (4) Post processing through strength reduction method for calculating factor of safety of the soil slope at various height and slope angles.
Step (5) Soil Nailing is used for strengthening of soil slop, concreting, and Geogrid strengthening is part of the process of re-determining the Factor of Safety of the soil slope in an area affected by subsidence or landslides.

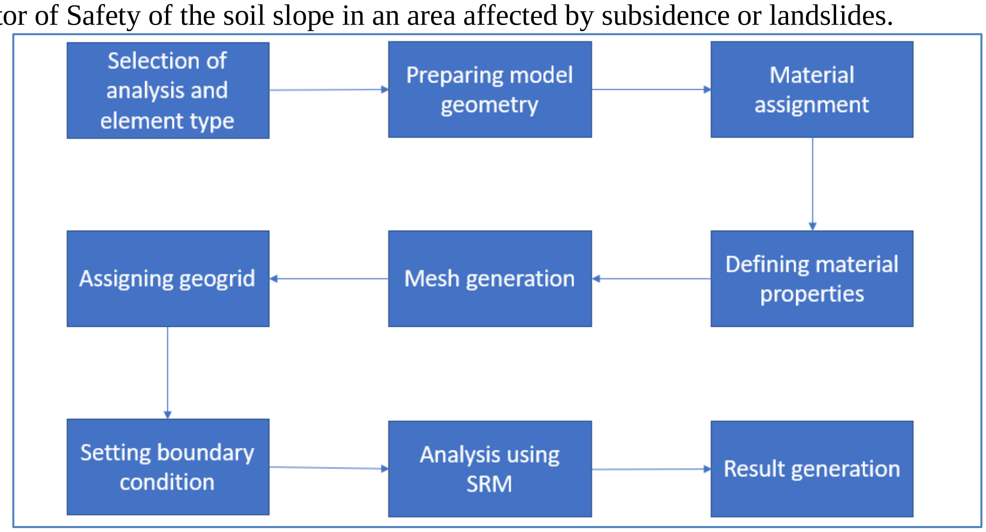

Figure 4 Flow chart showing process overview

The computation time is reduced after automating the numerical calculation which are highly accurate at the same time. The only disadvantage received while working through this software is that we need to deal with the inconstant units. The above flow chart in figure (4) explains sequential tasks performed in calculating factor of safety of a complex slope.
SRM outperformed (P.A. & D.V., 1999) (A., et al., 1999) as compared to other conventional methods in analyse for slope which are prone to failure. The two major draw backs which are identified while working with this method is first selecting the appropriate element size and second defining the suitable boundary conditions, but these drawbacks can be rectified by taking inputs from historical data and topographical details.

METHODOLOGY ADOPTED

The main objective of this chapter is to provide an overview of the methodology used to achieve all the sub-objective and final objective of the study in detail.

4.1 Model geometry

Model validation:

The results of the current study are compared to those of a previous study (Wulandari & Tjandra, 2015) that did not use geogrid. The reference paper's factory of safety (FOS) value was 1.35, and FOS for the validation of my model will be 1.59, as stated in the percentage error will be 11%.

The first stage in developing an embankment model is to define the geometry properties of the embankment, such as its height, slope, and crest width. The material qualities of the sandy and clayey layer soil (foundation) and the under-laying soil are provided in the second step.

The main model, with heights of 4.2, 8 and 14 metres, and crest widths of 16 metres, is constructed on a 21-meter embankment foundation with slopes of 28˚, 45˚, and 60˚. This embankment was strengthened using layers of geogrid of varying lengths along the length of the embankment from top to bottom. Geogrid vertical spacing varies between 0.457, 0.762, 1.066, and 1.371 metres. Modelling the traffic load was done using a variable surcharge of 20kN/m2, 50kN/m2, 80kN/m2, and 120kN/m2. (IRC , 2000). The effect of PET and PP geogrid on reinforced embankments was investigated. The identical model with tensile strength of 250kN/m is analysed using PET and PP geogrid samples. Furthermore, each layer of geogrid was supposed to have the same tensile strength and be arranged horizontally.

Based on the assumption that the foundation soil is strong enough to support the load from the higher structure, slope or shallow slope collapse will occur in the embankment structure. The MIDAS GTS NX slope stability software is used in this study to undertake analytical modelling of geogrid-reinforced slopes. Figures (5), (6), (7) illustrates the geometry.

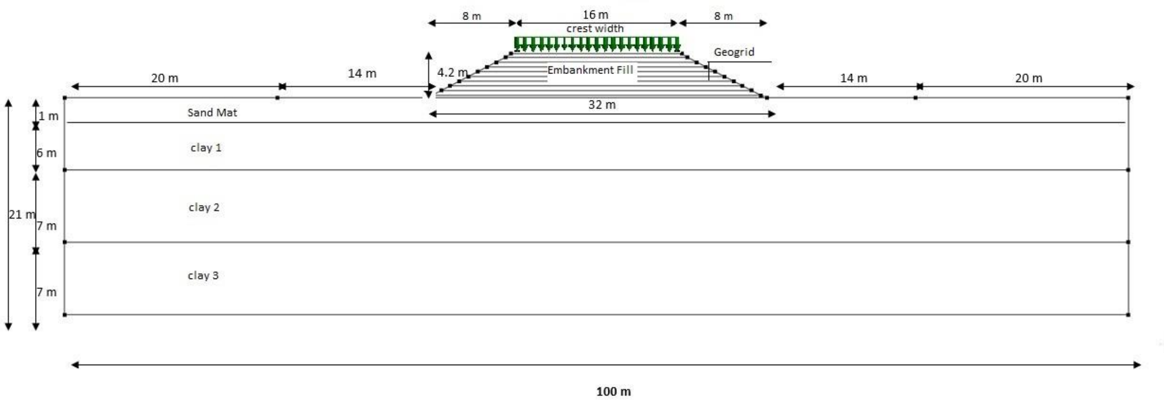

Figure 5 Model geometry at 28^{o} angle

Volume: 08 Issue: 11 | Nov- 2024 SJIF Rating: 8.448 ISSN: 2582-3930

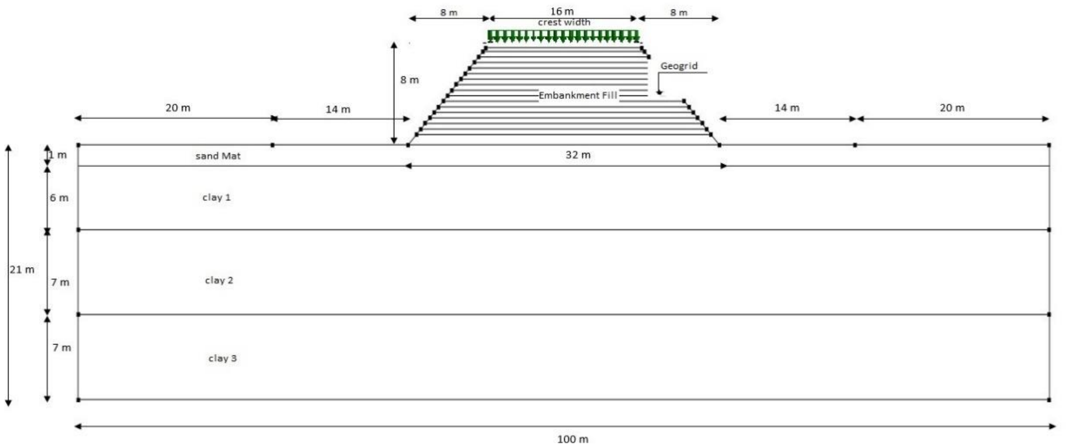

Figure 6 Model geometry at 45^o angle

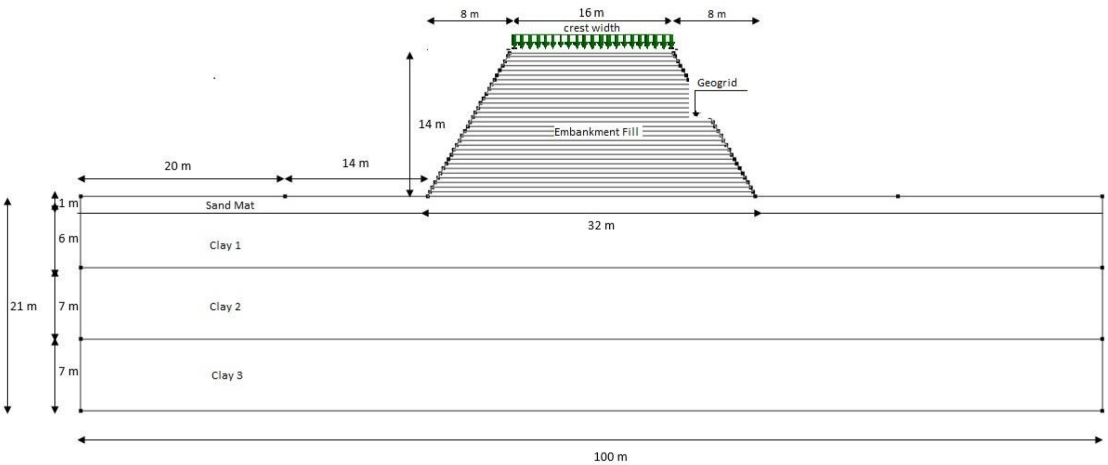

Figure 7 Model geometry at 60^o angle

Material Properties

The consolidation and time relative behavior of the sandy and clayey layer must be considered in analysis of the model, because under laying is relatively soft in monsoon. Two types of models were generated, first model is generated using clay, and embankment fill consisted well graded sand and second model were generated with sand, and embankment fill consisted well graded sand. The analysis uses where sand mat was model as drained condition and for the foundation clay soil is modelled undrained condition. The details of these models are presented in table 1 and table 2.

Material	E_{ref} (KN/m^2)	γ_{unsat} (KN/m^3)	γ_{sat} (KN/m^3)	C (KN/m^2)	Ø (**0**°)	Ψ (0˚)	ν
Embankment Fill	40000	17.5	23	5	32	3	0.28
Sand Mat	30000	18	23	1	33	3	0.28
Clay (1)	2000	16.6	17.31	47.01	1	0	0.32

Clay (2)	2000	16.6	17.31	33.02	1	0	0.32
Clay (3)	2000	16.6	17.31	12.01	1	0	0.32

Table 2 properties of clay model (P S. & D. Tjander, 2015)

Material	E_{ref} (KN/m^2)	γ_{unsat} (KN/m^3)	γ_{sat} (KN/m^3)	C (KN/m^2)	Ø (0°)	Ψ (0˚)	ν
Embankment Fill	40000	20	23	5	32	3	0.3
Sand Mat	30000	18	23	1	33	3	0.3
Sand (1)	2000	20	23	5	32	0	0.28
Sand (2)	2000	17.3	19	1.73	30	0	0.28

Table 3 properties of sand model (Jie, et al., 2007)

Material	E_{ref} (KN/m^2)	γ_{unsat} (KN/m^3)	γ_{sat} (KN/m^3)	ν
Geogrid	950000	0.5	0.5	0.35

Table 4 properties of geogrid (Mittal & Bhardwaj, 2020)

RESULTS AND DISCUSSION

All of the results produced from the methods described in the previous part have been addressed in this chapter.
To analyse the reinforced road embankment, we use three different types of angles 28˚, 45˚ & 60˚ respectively. The all three types of embankments are analysed without geogrid, and it was found that FOS value decrease with increase in load than embankments is reinforced with geogrid for the analysis. The graph is drawn between FOS and spacing for all three cases, and it was found that with increasing in spacing FOS is decreases but decreases in FOS is not significant for sand embankment material model.

5.1 Sand model:

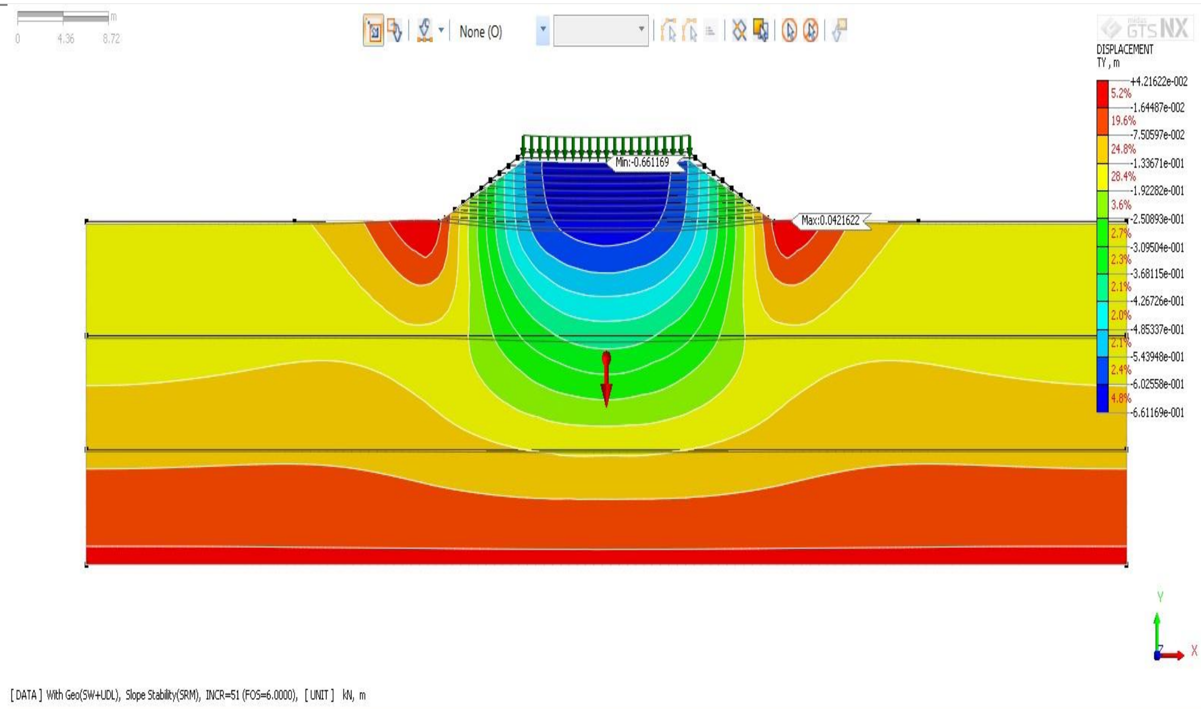

Figure 8 Deformation analysis of sand model at 28˚embankment angle

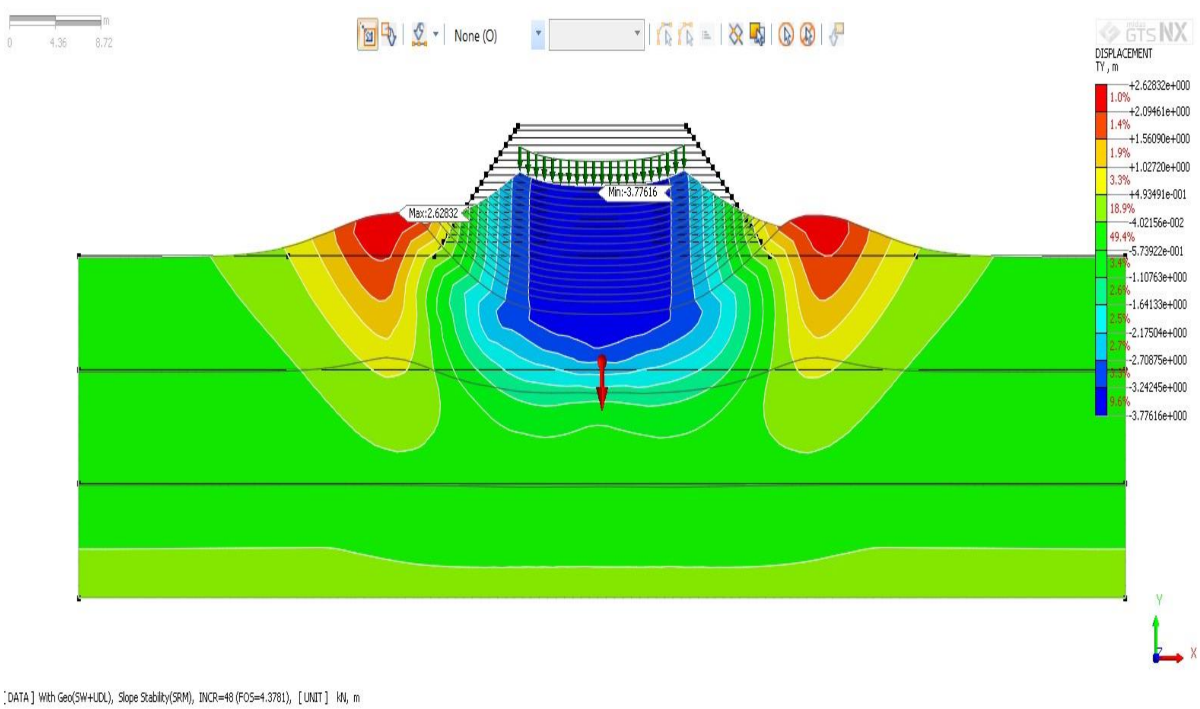

Figure 9 Deformation analysis of sand model at 45˚embankment angle

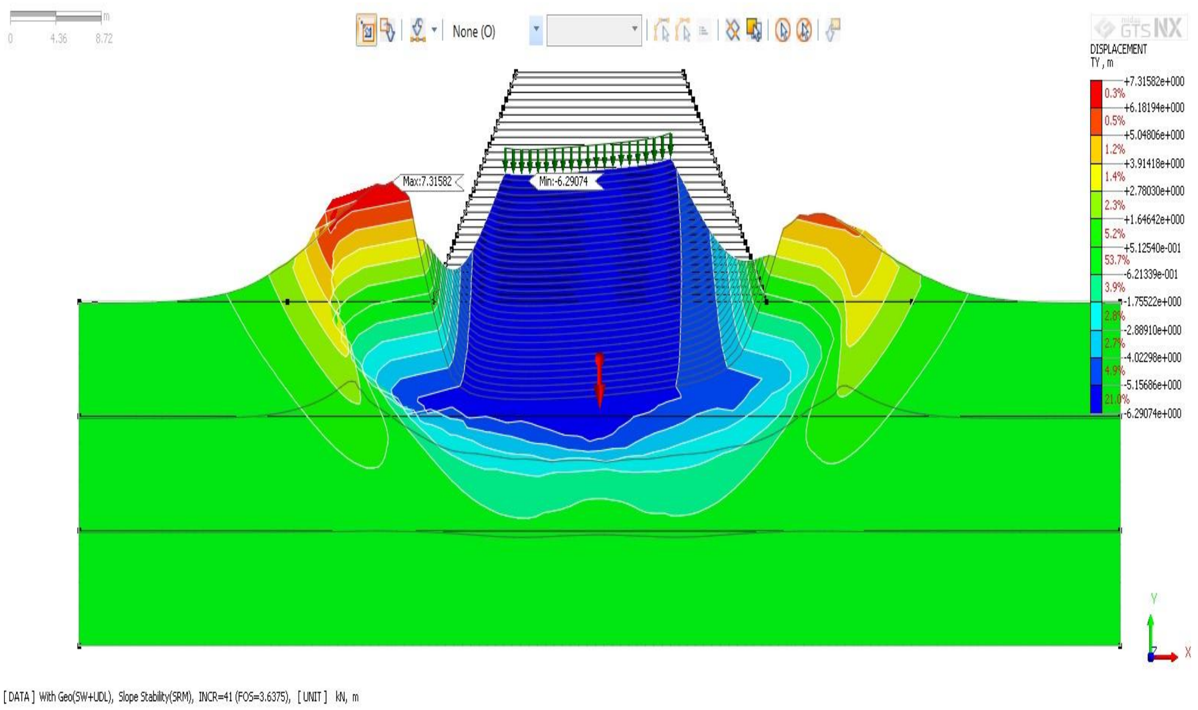

Figure 10 Deformation analysis of sand model at 60˚embankment angle

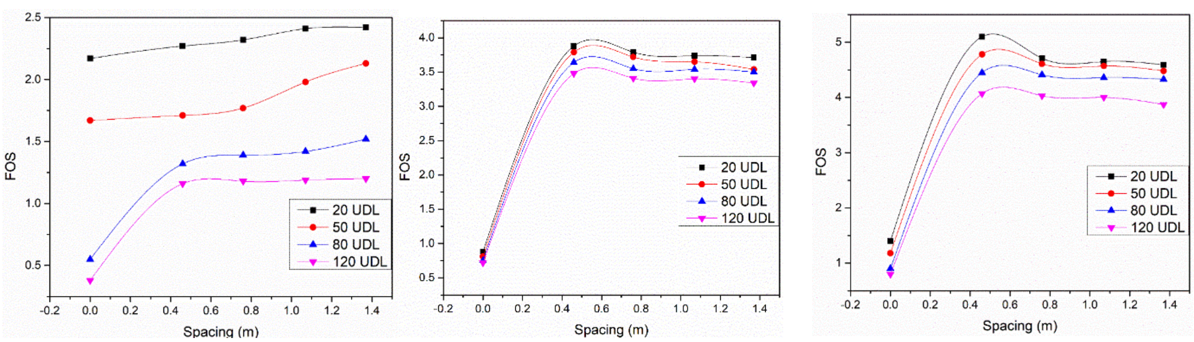

Figure 11 Analysis of FOS sand model at 28˚, 45˚ and 60˚ embankment angle

Initially when the plot between FOS and spacing were observe figure (8) is analysed without geogrid, it is observed that the FOS value is same at different angle at varying load. When the same plot is analysed with geogrid, it is observed that as spacing between geogrid as well as loading is increased, FOS gets reduced compared to less spacing. Same trend is followed at different angle.

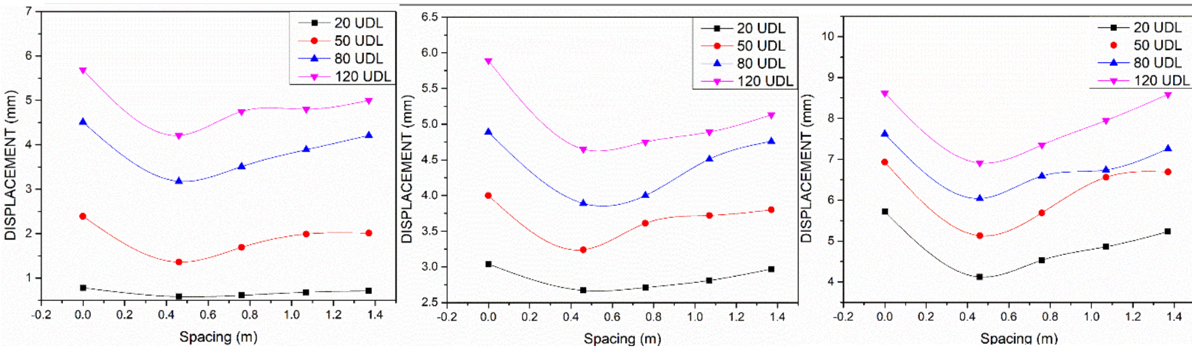

Figure 12 Analysis of displacement of top geogrid layer of sand model at 28˚, 45˚ and 60˚ embankment angle

When plot between displacement and spacing as shown in figure (9) is analysed, it is observed that without geogrid the displacement is same at all embankment angle but as geogrid is placed between embankment, the displacement increases with increase in spacing between geogrid at varying angle as well as load. Also, with increase in embankment angle, displacement is also increased.

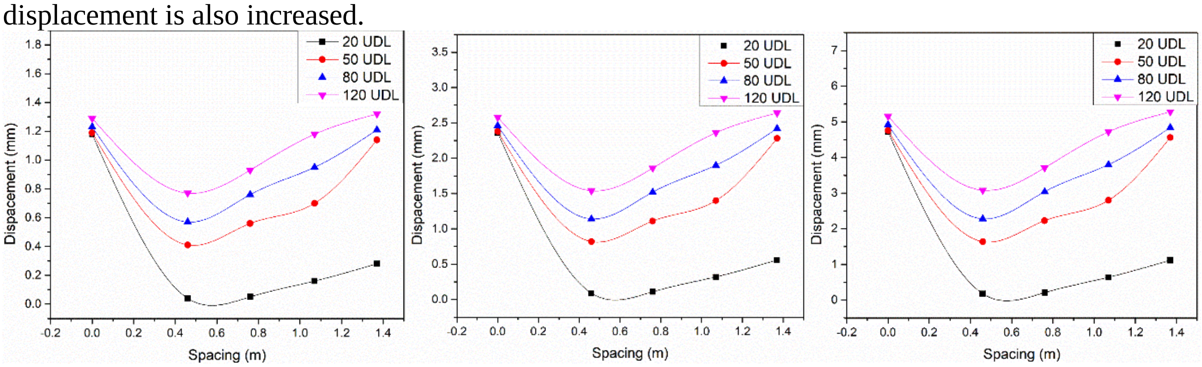

Figure 13 Analysis of total displacement of sand model at 28˚, 45 ˚ & 60 ˚ angle

When plot between total displacement and spacing as shown in figure (10) is analysed, it is observed that without geogrid the displacement is same at all embankment angle but as geogrid is placed between embankment, total displacement also increases with increase in spacing between geogrids. Also, with increase in embankment angle, total displacement is also increased.

Hence, it can be concluded that when embankment angle, and spacing of geogrid is increased, total displacement also increases.

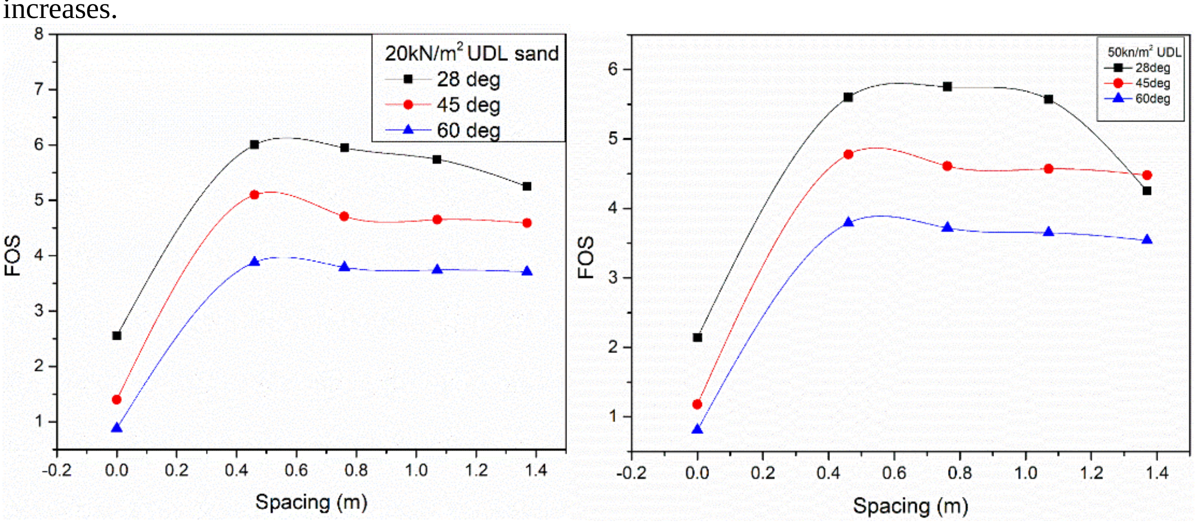

Figure 14 Sand model comparison of FOS seen on different embankment angle (28˚ (black), 45˚(red) & 60˚(blue) with 20kN/m², 50kN/m²

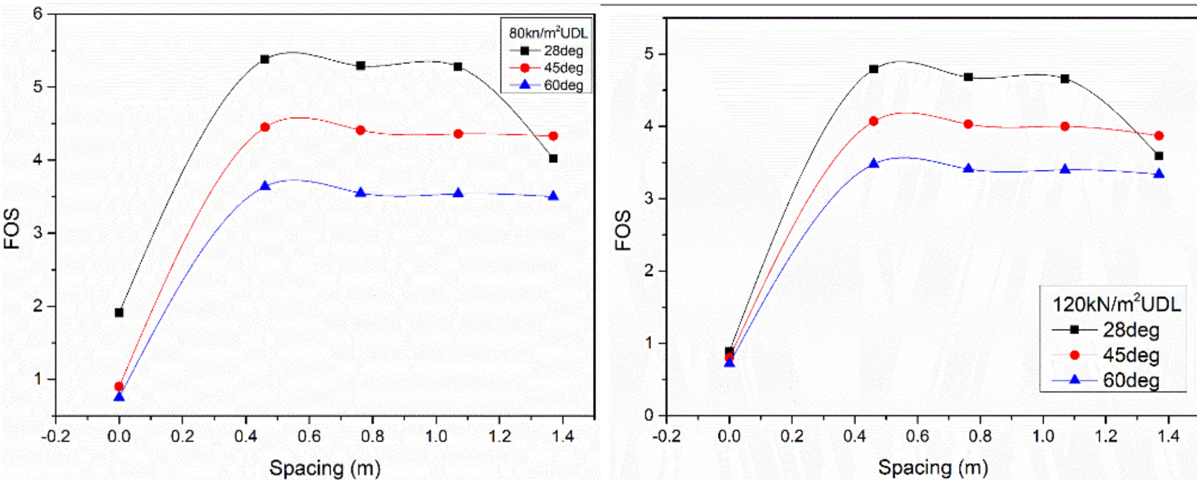

Figure 15 Sand model comparison of FOS seen on different embankment angle (28˚ (black), 45˚(red) & 60˚(blue) with 80kN/m2, 120kN/m2

When the comparison plot between FOS and spacing as shown in figure (11) and (12) is analysed, it is observed that at constant loading of 20kN/m^2, 50kN/m^2, 80kN/m^2, and 120kN/m^2, the FOS value is same without geogrid. When geogrid is placed between embankment, the FOS decreases with increase in spacing between geogrids. Also, with increase in embankment angle, FOS further decreases.

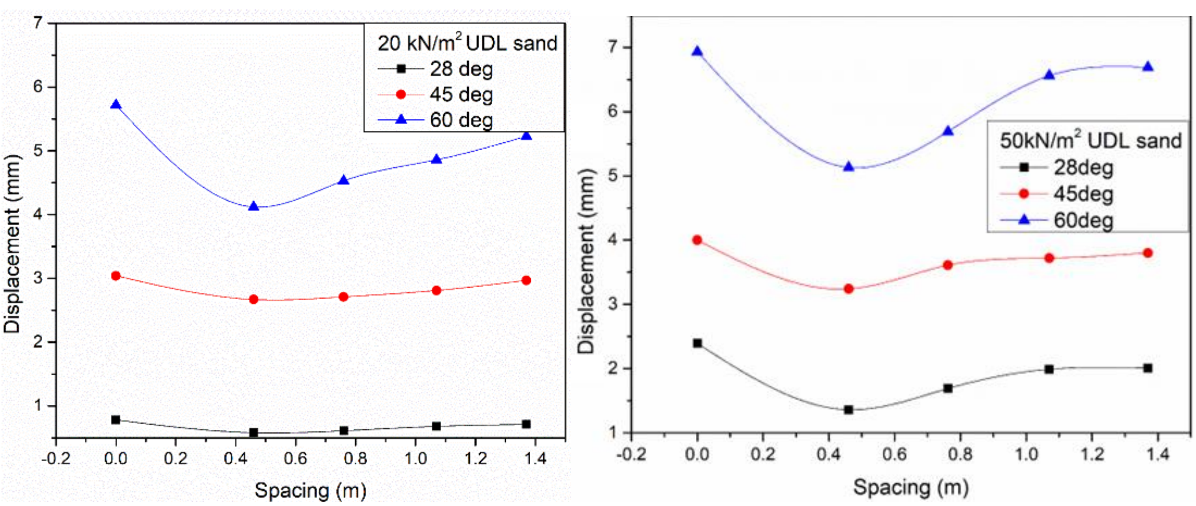

Figure 16 Sand model comparison of displacement seen on different embankment angle (28˚ (black), 45˚(red) & 60˚(blue) with 20kN/m^2, 50kN/m^2

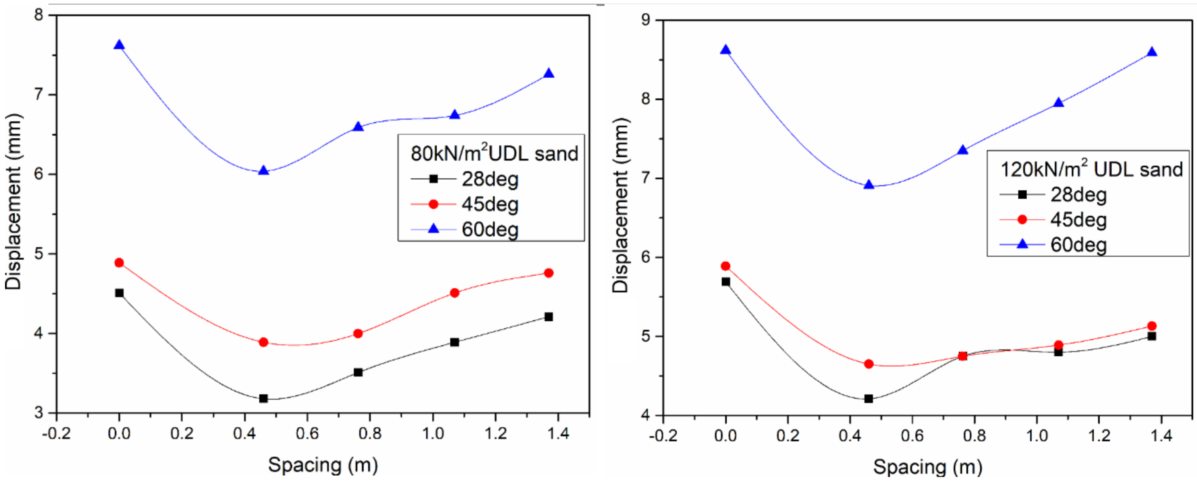

Figure 17 Sand model comparison of displacement seen on different embankment angle (28˚ (black), 45˚(red) & 60˚(blue) with 80kN/m²and 120kN/m²

When the comparison plot between displacement and spacing as shown in figure (13) and (14) is analysed, it is observed that at constant loading of 20kN/m², 50kN/m², 80kN/m²and 120kN/m², the displacement value is same without geogrid at all angles. When geogrid is placed between embankment, the displacement value increases with increase in spacing between geogrids. Also, with increase in embankment angle, displacement further increases.

5.2 Clay model:

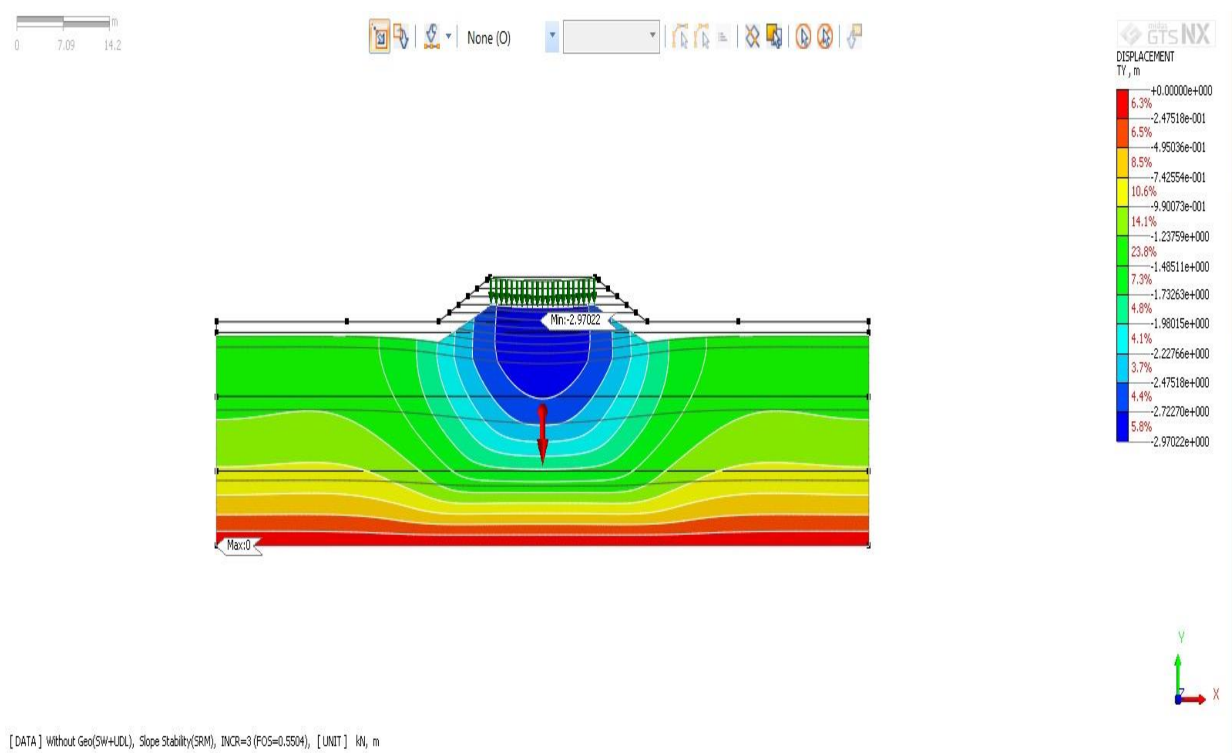

Figure 18 Deformation analysis of clay model at 28˚embankment angle

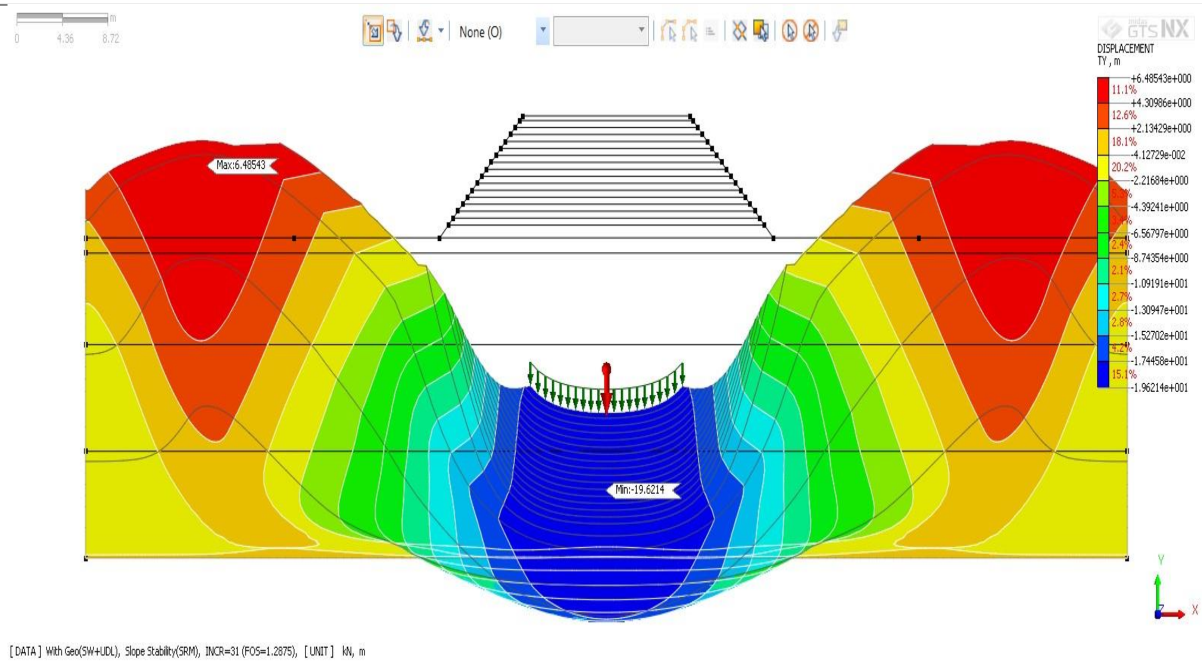

Figure 19 Deformation analysis of clay model at 45˚embankment angle

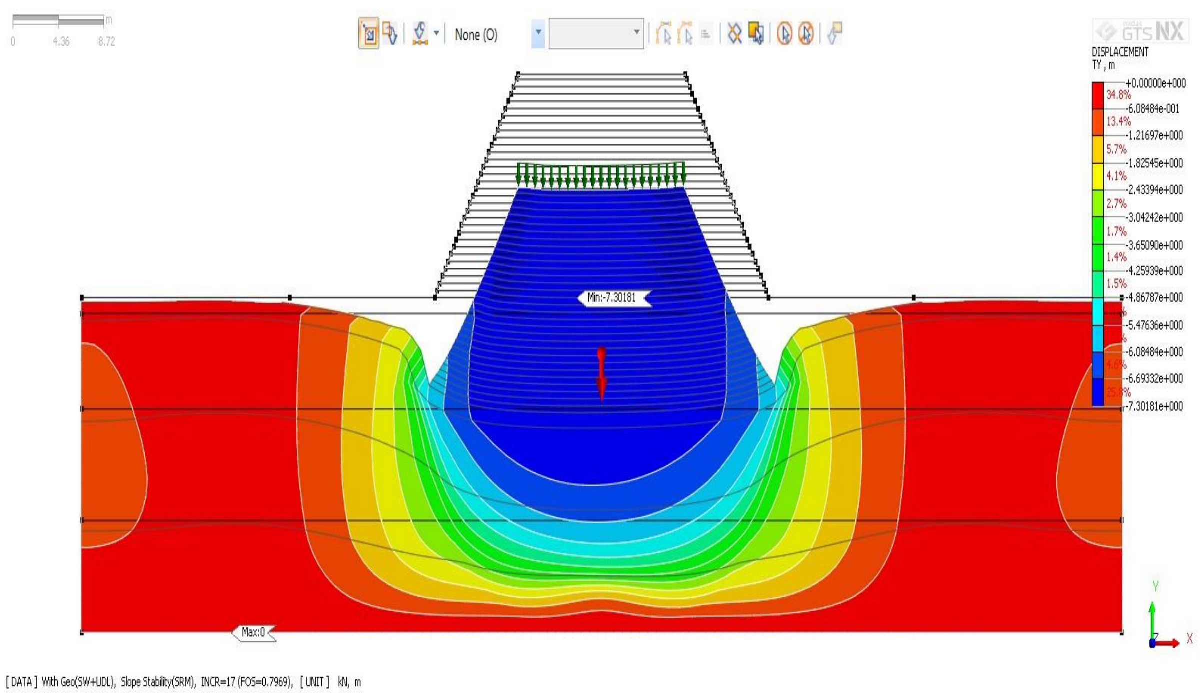

Figure 20 Deformation analysis of clay model at 60˚embankment angle

International Journal of Scientific Research in Engineering and Management (IJSREM)
Volume: 08 Issue: 11 | Nov- 2024 SJIF Rating: 8.448 ISSN: 2582-3930

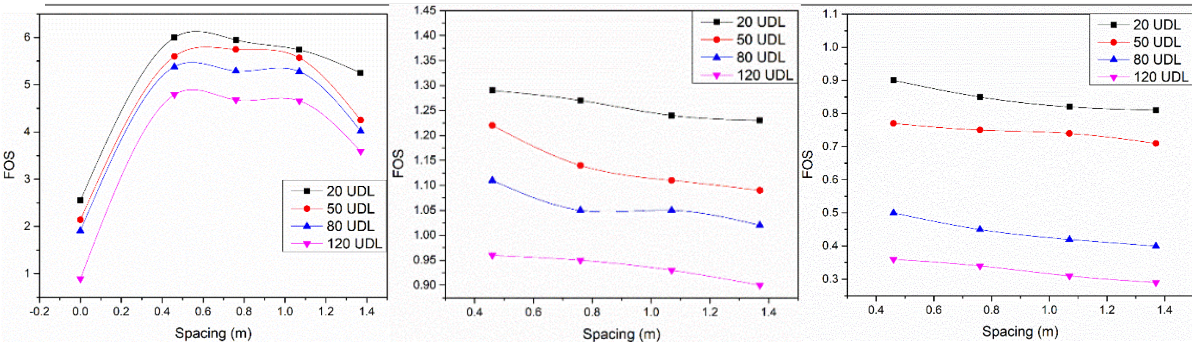

Figure 21 Analysis of FOS clay model at 28˚, 45˚ and 60˚ embankment angle

Initially when the plot between FOS and spacing is shown in figure (15) is analysed without geogrid, it is observed that the FOS value is same at 28˚ embankment angle but at 45˚ and 60˚ embankment angle, FOS value came to be less than 0.6 which is not considerable. When the same plot is analysed with geogrid, it is observed that as spacing between geogrid as well as loading is increased, FOS gets reduced compared to less spacing at all angles. Compared to sand model, the FOS decreases is around two times higher for clay model at constant angle

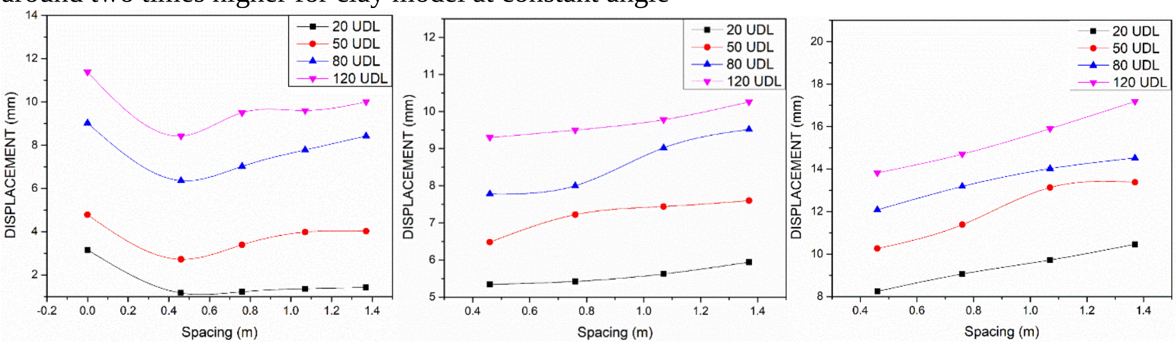

Figure 22 Analysis of displacement of top geogrid layer of clay model at 28˚, 45˚ and 60˚ embankment angle

When plot between displacement and spacing as shown in figure (16) is analysed, it is observed that without geogrid the displacement is same at 28˚ embankment angle but at 45˚ and 60˚ embankment angle, displacement value is not obtained. When geogrid is placed between embankment, the displacement increases with increase in spacing between geogrid at varying angle as well as load. Also, with increase in embankment angle, displacement is also increased.

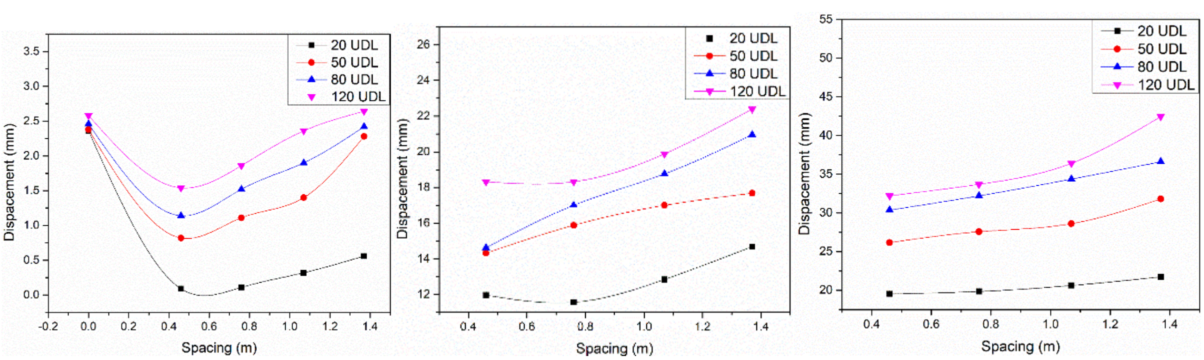

Figure 23 Analysis of total displacement of clay model at 28˚, 45 ˚ & 60 ˚ angle

When plot between total displacement and spacing as shown in figure (17) is analysed, it is observed that without geogrid the displacement is same at 28˚ embankment angle but at 45˚ and 60˚ embankment angle, displacement value is not obtained. When geogrid is placed between embankment, total displacement also increases with increase in spacing between geogrids. Also, with increase in embankment angle, total displacement is also increased.
Hence, it can be concluded that when embankment angle, and spacing of geogrid is increased, total displacement also

increases.

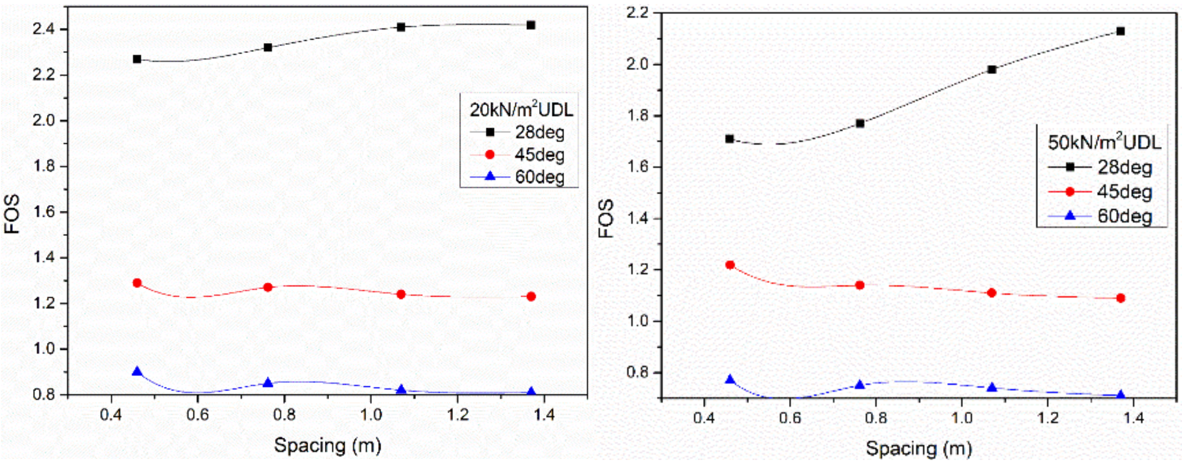

Figure 24 Clay model comparison of FOS seen on different embankment angle (28˚ (black), 45˚(red) & 60˚(blue) with 20kN/m^2, 50kN/m^2

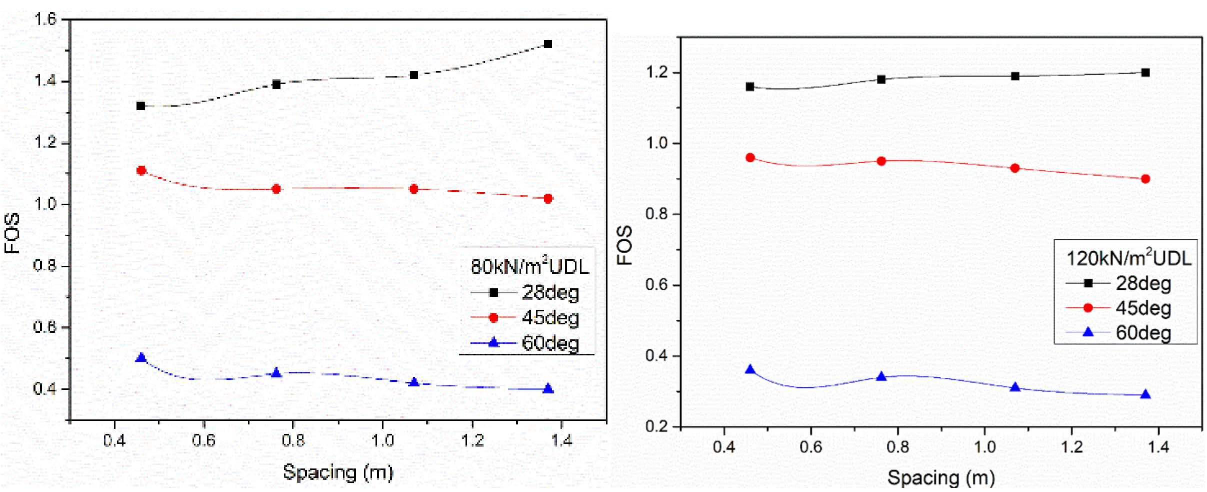

Figure 25 Clay model comparison of FOS seen on different embankment angle (28˚ (black), 45˚(red) & 60˚(blue) with 80kN/m^2, 120kN/m^2

When the comparison plot between FOS and spacing as shown in figure (18) and (19) is analysed, it is observed that at constant loading of 20kN/m^2, 50kN/m^2, 80kN/m^{2}and 120kN/m^2 the FOS value is not obtained without geogrid. When geogrid is placed between embankment, the FOS decreases with increase in spacing between geogrids. Also, with increase in embankment angle, FOS further decreases.

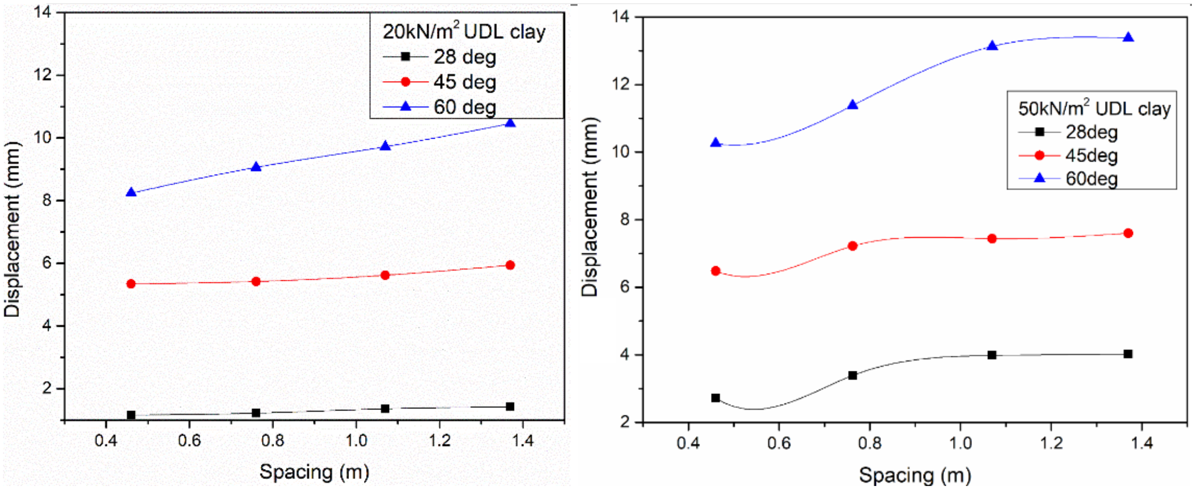

Figure 26 Clay model comparison of displacement seen on different embankment angle (28˚ (black), 45˚(red) & 60˚(blue) with 20kN/m^2, 50kN/m^2

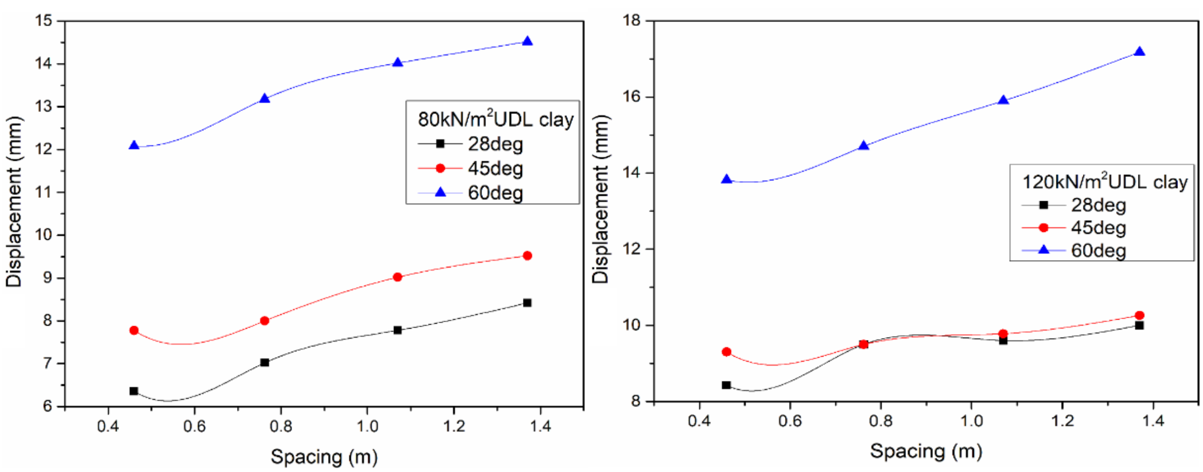

Figure 27 Clay model comparison of displacement seen on different embankment angle (28˚ (black), 45˚(red) & 60˚(blue) with 80kN/m^2 and 120kN/m^2

When the comparison plot between displacement and spacing as shown in figure (20) and (21) is analysed, it is observed that at constant loading of 20kN/m^2, 50kN/m^2, 80kN/m^2 and 120kN/m^2, the displacement value is not obtained without geogrid at all angles. When geogrid is placed between embankment, the displacement value increases with increase in spacing between geogrids. Also, with increase in embankment angle, displacement further increases.

Future scope

More research is needed to build a road embankment stability prediction system that takes into account settlement, soil bearing capacity, and slope stability based on soil parameters.

This is an essential topic for future research in order to produce new guidelines with crucial, safe, and appropriate side slope requirements. Furthermore, the link between crest width, side slope, and embankment height may be studied in the future in order to produce a defined level or value range that meets critical, safe, and acceptable requirements.

CONCLUSION

Following conclusions were made after analysing all the results using methodology explained earlier-

i. As the height of embankment increases, safety factor (FOS) decreases. The embankment is analysed by fixing the load at constant angle with and without geogrid. It is observed that there is considerable increase in FOS with addition of geogrid in embankment. Also, if the spacing of geogrid is increased, some decrease in FOS is observed.

ii. On analysing three embankments at angle of 28˚, 45˚, and 60˚ at 20 KN/m^2 load, it is observed that on increasing the spacing between geogrids, displacement increased significantly at 60˚ angle but at 28˚ and 45˚ the increase in displacement is very minimal compared to 60˚. At fixed angle of embankment with higher load, the influence of spacing between geogrid on displacement is found to be more significant.

iii. Embankments were made with and without geogrid, and it is obvious that the geogrid embankment provides more consistent outcomes.

iv. When the geogrid spacing is increased, the factor of safety (FOS) decreases as the load increases.

v. When the embankment angle and geogrid spacing are both increased, the displacement increases as well.

vi. When the embankment angle is raises, deformation increases, and the safety factor decreases.

vii. When comparing the stability of 28˚ embankment angles, the stability of 60˚ embankment angles is lower.

viii. The stability of the embankment rises as the load on it increases. As the geogrid spacing is increased, the embankment's stability decreases.

ix. The capacity to identify by exposing crucial failure in real time, highlighting existing shear and displacement values could be extremely useful in reducing the threat of slope failures in our study areas. MIDAS GTS is a slope stabilisation software that is rising in popularity as a tool for determining slope stability.

REFERENCES

A., D., W.H., R. & E.M., D., 1999. “Slope Stability Analysis by Strength Reduction”. *Geotechnique Vol.,* 49(6), pp. 835-840,.

Akbas, B., 2015. Probabilistic slope stability analysis using limit equilibrium, finite element and random finite element methods.. *Middle East Technical University..*

Alemdag, et al., 2015. Utilization of the limit equilibrium and finite element methods for the stability analysis of the slope debris: an example of the Kalebasi district (NE Turkey).. *Journal of African Earth Sciences,,* Volume 106, pp. 134-146.

Awalla, H., Taher,, H. , A. & Mawlood,, Y. I., 2020. Effect of Fixed-Base and Soil Structure Interaction on the Dynamic Responses of Steel Structures.. *International Journal of Emerging Trends in Engineering Research,*, 8(9), pp. 6298-6305.

Bacic, B. & Uljarevic, M., 2014. Slope Stability Analysis. *University of Novi Sad.*

Barqawi, M. A. et al., 2021. Polymer Geogrids: A Review of Material, Design and Structure Relationships. *MDPI,* Volume 16, p. 14.

D. T., B. & C., T., 2008. 2D and 3D Numerical Simulations of reinforced Embankment on Soft Ground,. *Geotextiles and Geomembranes,* Volume 26, pp. 39-55.

D., A., S., L., O., J. E. & M., W., 2014. An Original Testing Apparatus for Rapid Pull-Out Test,. *Civil Engineering Dimension,* Volume 16, pp. 61-67.

Dennen, T. B., Pham, V. L. & B.R., S. M., 2002. A case study of geotextile-reinforced embankment on soft ground. *Geotextile and Geomembranes,* Volume 20, pp. 343-365.

F., K. et al., 2013. Simulation of geogrid reinforced embankment on soft ground using Plaxis,. *APCBEE Proceedia,* Volume 5, pp. 152-156.

Fernando Alonso, 2013. “Finite Element Modeling For Civil Engineering”. *The University of Sydney,.*

Gor, M., 2021. Limit denge analizi (Bishop Yöntemi) ile kütle hareketinin mekanizması ve önlem yapısının analizi: Van ili örneği.. *Gümüşhane Üniversitesi Fen Bilimleri Enstitüsü Dergisi,,* 11(2), pp. 597-608.

GTS, M., 2014. Verification &Application Manual.

H. Jerry Qi, 2006. “Finite Element Analysis". *University of Colorado Boulder,.*

Hamdhan, I. N., 2013. Slope Stability Analysis with the Finite Element Method. *Itenas Library, National Institute of Technology, Bandung, Indonesia,.*

Hammah, R., 2005. The Shear Strength Reduction Method for the Generalized Hoek-Brown Criterion. *American Rock Mechanics Association.*

IRC , 6., 2000. "Standard specification and code of practice for road bridges".

J. M., V., A. K., D. & C. H., S., 2013. Analysis of geotextile reinforced embankment on different subsoil condition,. *Inernational Journal of Scientific & Engineering research* , 4(5), pp. 41-44.

Jie, H., Sadik , O., Robert, L. P. & Jie, H., 2007. Numerical analysis of foundation columns to support widening of embankments,. *Computer and geotechnics,* Volume 34, pp. 435-448.

kevadiya, M. & Vaidya, H. A., 2013. 2D ANALYSIS OF NACA 4412 AIRFOIL. *International Journal of Innovative Research in Science, Engineering and Technology,* , 2(5), pp. 1686-1691.

M., S., F., K. & A., S., 2010. Assessment of geotextile reinforced embankment on soft clay soil,. *The 1st International applied Geological Congress, Iran,* pp. 1779-1784.

Mesut, G., Nichirvan, R. T. & Halmat, A. A., 2022. Effect of geogrid inclusion on the slope stability. *5th international european conference on interdisplinary scientific research,,* pp. 28-29.

MIDAS, G., 2014. "Verification & Application Manual".

Mittal, S. & Bhardwaj, A., 2020. Performance Behavior of Geogrids at Interface of Ballast. *Indian Geotech J,* Volume 5, pp. 753-765.

Mwasha, A., 2009. Modelling Limited Life geotextiles For reinforcing An Embankment on the soft soil. *West indian journal of engineering,* Volume 31, pp. 1-9.

P S., W. & D. Tjander, 2015. Analysis of geotextile reinforced road embankment using plaxis 2d. *The 5th International conference of Euro Asia Civil Engineering Forum (EACEF-5) Surabaya* , Volume 125, pp. 121-131.

P. S., W. & and D. Tjandra, 2006. Determination of optimum tensile Strength of Geogrid reinforced embankment,. *International Civil Engineering Conference "Towards Sustainable Civil Engineering Practice",,* pp. 187-193.

P.A., L. & D.V., G., 1999. "Slope Stability Analysis by Finite Elements",. *Geotechnique Vol.,,* 49(3), pp. 387-403.

Tarun, G. & Vinod K., S., 2017. A review on slope stability analysis by strength reduction method using MIDAS GTS. *International Journal of innovative research in science engineering and technology* , 6(8), pp. 2347-6710.

Wulandari, P. S. & Tjandra, D., 2015. Analysis of geotextile reinforced road embankment using PLAXIS 2D. *Procedia Engineering,* Volume 125, pp. 358-362.